Bond particle theory for the pseudogap phase of underdoped cuprates

R. Eder ⬡

Karlsruher Institut für Technologie, Institut für Festkörperphysik, 76021 Karlsruhe, Germany

We present a theory for the lightly doped t-J model that is of possible relevance for the normal state of underdoped cuprates. Starting from an arbitrary dimer covering of the plane, an exact representation of the t-J Hamiltonian in terms of bond bosons and fermions can be derived. Since all dimer coverings must give identical results for observable quantities, we construct an approximate but translationally invariant Hamiltonian by averaging the bond particle Hamiltonian over all possible dimer coverings. Treating the resulting Hamiltonian in the mean-field approximation, we find Fermi pockets centered near $(\pi/2, \pi/2)$ with a total area of $x/2$ (with x the hole concentration) and a gapped spin-wave-like band of triplet excitations.

I. INTRODUCTION

Copper-oxide-based superconductors have a phase diagram that is similar to a large number of heavy-fermion compounds and the iron pnictide superconductors [1]. In all these materials, a phase transition occurs at zero temperature as a function of some control parameter that is surrounded by a superconducting dome. In the cuprates, the control parameter is the hole concentration x in the CuO_2 planes. However, whereas the phase on the overdoped side of the transition appears to be a normal metal, albeit with correlation-enhanced effective mass, the underdoped phase—the so-called pseudogap phase—is not well understood. To begin with, we briefly summarize some experimental results for this phase.

Below the pseudogap temperature T^*, which decreases monotonously with x, angle-resolved photoelectron spectroscopy (ARPES) shows Fermi arcs and a pseudogap [2–4], i.e., unlike what is expected for the hole-doped density functional band structure, the quasiparticle band does not reach the chemical potential μ in a sizable range in $\boldsymbol{k}$-space around $(\pi, 0)$. One possible explanation would be that the Fermi arc really is one-half of an elliptical or semielliptical hole pocket that is centered near $(\frac{\pi}{2}, \frac{\pi}{2})$, formed by a band with weak dispersion along $(0, \pi) \rightarrow (\pi, 0)$. To reconcile this interpretation with experiment, one has to make the additional assumption that the ARPES weight of the quasiparticle band has a strong $\boldsymbol{k}$-dependence and drops sharply to almost zero upon crossing a line in $\boldsymbol{k}$-space that roughly corresponds to the antiferromagnetic zone boundary, so that only the part of the pocket facing (0,0) can be resolved, whereas the part facing (π, π) has too low spectral weight. In fact, much the same behavior is indeed observed in insulating cuprates [5,6], where this phenomenon has been termed the remnant Fermi surface. In the underdoped compounds, the drop of spectral weight would have to be even more pronounced, however, to be compatible with experiment.

The length of the Fermi arcs is independent of temperature [7,8] up to T^*, as expected for a true Fermi surface. At T^* the arcs disappear abruptly and ARPES apparently shows the free-electron Fermi surface. The length of the arcs increases with x [8,9], which suggests that the carriers that form the pockets are the doped holes. A somewhat unusual feature is the temperature dependence of the dispersion, i.e., while the arc length is temperature-independent, the dispersion along $(0, \pi) \rightarrow (\pi, 0)$ flattens with increasing temperature [8,10], so that the pseudogap seems to close with increasing temperature. It is plausible that the motion of the doped holes through the "spin background" will be influenced by the spin correlations of the latter. Since these change with temperature, a temperature dependence of the hole dispersion is not entirely unexpected.

The asymmetry of the spectral weight around $(\frac{\pi}{2}, \frac{\pi}{2})$, which gives rise to the remnant Fermi surface in the insulating compounds, is reproduced by exact diagonalization of the half-filled t-J or Hubbard model [11]. It can be explained by the coupling of the photohole to the quantum spin fluctuations of the Heisenberg antiferromagnet or t-J model [12], further enhanced by the coupling to charge fluctuations in the Hubbard model [13].

Further insight can be gained from thermodynamic and transport properties. Thereby, an extra complication has to be taken into account, namely the tendency of underdoped cuprates to form inhomogeneous states with charge-density-wave (CDW) order with ordering wave vector $\mathbf{q}_{\text{CDW}} = (q, 0)$, the precise nature of which depends on the material. It may be combined with spin order [14], "checkerboard order" [15], or CDW order without spin order [16]. Typically these ordered states are observed at low temperatures and in a certain doping range $[x_{\min}^{\text{CDW}}, x_{\max}^{\text{CDW}}]$. When this is taken into account, various results indicate that the underdoped cuprates are Fermi liquids. The charge carrier relaxation rate τ^{-1} extracted from the optical conductivity of various underdoped cuprates (with $x \approx 0.1$) has a quadratic dependence on both frequency ω and temperature T [17]. For compounds with $x < 0.15$ and for temperatures below T^*, the dc-resistivity ρ varies with temperature as $\rho = AT^2$ with an x-dependent constant A [18,19], although this behavior is masked at lower temperatures by CDW order, superconducting fluctuations, or localization [19]. This is also consistent with the variation of

the Hall angle with temperature as $\cot(\Theta_H) \propto T^2$ [18]. The Wiedemann-Franz law is obeyed [20], as is Kohler's rule [21]. The entropy S and the magnetic susceptibility χ are related over a wide doping range by $S = aT\chi$, with a the Wilson ratio for spin-$\frac{1}{2}$ fermions [22]. This is expected for a free Fermi gas because S/T and χ probe the fermionic density of states (DOS) around μ by similar weighting functions so that the proportionality should hold even for a structured or temperature-dependent DOS [22].

The one unusual feature, however, is the x-dependence of transport quantities. It is found that $A \propto x$, as would be expected from Drude theory for a Fermi gas with carrier density $n_c = x$, and the value of A per CuO$_2$ plane is material-independent [19]. For larger $x \approx 0.2$, and when superconductivity is suppressed by a magnetic field, the carrier density inferred from the $T \to 0$ limiting values of ρ shows a sharp crossover at a material-dependent $x^* \approx 0.2$ from $n_c = 1 + x$ for $x > x^*$ to $n_c = x$ for $x < x^*$ [23,24]. The carrier density can also be inferred from the Hall constant R_H, but this is complicated by the occurrence of CDW order. In the absence of CDW order, $R_H > 0$ [23,24], as expected for holelike carriers. From measurements of R_H at sufficiently high temperatures, where there is neither superconductivity nor CDW order, one infers $n_c = x$ at $x \leqslant 0.1$ [25–27]. For larger x and when superconductivity is suppressed by a magnetic field, n_c inferred from R_H again crosses sharply from $n_c = 1 + x$ to $n_c = x$ at the same x^* where this occurs for ρ [23,24]. Thereby, x^* coincides with the "critical doping" where $T^*(x) \to 0$ as inferred from a variety of physical properties [28]. It is found that $x^* > x_{\max}^{\mathrm{CDW}}$ so that the crossover in the x-dependence of n_c cannot be related to CDW order [23,24], which can also be seen from the fact that for $x < x_{\min}^{\mathrm{CDW}}$ the behavior $n_c = x$ is recovered [23,24]. In the CDW-ordered state itself, quantum oscillations [29–31] and the quadratic temperature dependence of ρ [32] confirm the Fermi-liquid nature of the ground state, whereas the negative R_H suggests the presence of electron pockets [33], likely caused by a reconstruction of the hole pockets. The observation of spin zeros in the angular dependence of the quantum oscillations suggests that the carriers are spin-$\frac{1}{2}$ fermions [34]. The wave vector $\mathbf{q}_{\mathrm{CDW}}$ of the CDW modulation varies with x, and this variation is consistent with the assumption that $\mathbf{q}_{\mathrm{CDW}}$ corresponds to the nesting vector connecting the tips of the Fermi arcs [35] along the direction $(\pi, 0) \to (0, \pi)$. This is to be expected in the hole pocket picture because for a band with weak dispersion along $(\pi, 0) \to (0, \pi)$, the tips would be the part of the Fermi surface with the lowest Fermi velocity and hence the highest density of states. Generally, assuming that the holes rather than the electrons are the mobile fermions, one would have a system with a low density of carriers with high effective mass, and the average energy of delocalization would be further reduced by the fact that there are four equivalent pockets so that the Fermi energy is reduced by a factor of 4. Such a system may well be susceptible to charge ordering due to long-ranged Coulomb interaction. Lastly, the Drude weight in the optical conductivity is $\propto x$ [17,27], again consistent with $n_c = x$. The effective mass, as inferred from n_c and the optical sum rule, is practically independent of doping over the underdoped region, and in fact also the antiferromagnetic phase [27].

A simple and unifying interpretation for a large body of ARPES and transport experiments on underdoped cuprates thus would be that below $T^*(x)$ these compounds are Fermi liquids formed by spin-$\frac{1}{2}$ fermions that correspond to the doped holes. The Fermi surface takes the form of hole pockets centered near $(\frac{\pi}{2}, \frac{\pi}{2})$ and with a "dark side" toward (π, π). This is also consistent with exact diagonalization studies for the t-J model, which show that for $x \approx 0.1$ the Fermi surface takes the form of hole pockets [36] and that the low-lying eigenstates can be mapped one-to-one to those of weakly interacting spin-1/2 fermions corresponding to the doped holes [37]—which is the defining property of a Fermi liquid.

The situation is very different for overdoped compounds where at low temperature ARPES [38–40], magnetoresistance [41], and quantum oscillations [42] show a free-electron-like Fermi surface that takes the form of a 3D hole barrel around (π, π) and covers a fraction of the Brillouin zone of $(1 + x)/2$. Consistent with the observation of quantum oscillations, the transport properties are Fermi-liquid-like [43]. Such a Fermi surface is expected in the limit of small electron density, $x \to 1$, so that the range of applicability of this limit appears to extend down to x^*. This is also consistent with exact diagonalization studies of the dynamical spin and density correlation functions in the t-J model, which indicate a transition to a more conventional renormalized free-electron Fermi surface at around $x = 0.25$ [44,45].

Taken together, the above experimental results suggest that the zero-temperature phase transition in the cuprates at x^* corresponds to the transition between the two types of Fermi surfaces: from pockets formed by the holes doped into the lower Hubbard band for $x < x^*$, to a more conventional Fermi liquid with correlation-enhanced band mass for $x > x^*$. While the latter phase probably may be adequately described by a Gutzwiller-projected Fermi sea, the phase realized for $x < x^*$ is more elusive, and it is the purpose of this paper to describe a theory that can describe it. The goal of this paper, therefore, is to develop a theory for the doped, para-magnetic Mott-insulator that is compatible with the scenario suggested by the above experimental results: a translationally invariant state without any type of order but with short-range antiferromagnetic spin correlations, which is a Fermi liquid of spin-$\frac{1}{2}$ fermions that correspond to the doped holes rather than the electrons, so that the volume of the Fermi surface is proportional to x, rather than $1 - x$. As will be seen below, the bond particle theory, which was used initially for the study of spin systems [46], is particularly suited to do so because it contains the right types of elementary excitations as its "natural particles."

Theoretically, a hole pocket Fermi surface can always be produced by backfolding a free-electron-like Fermi surface assuming some order parameter with wave vector (π, π) [47,48]. However, no evidence for such an order parameter has been observed so far. Constructing a theory that gives a Fermi surface with a volume proportional to x without invoking backfolding of a free-electron Fermi surface is not achieved easily. Various authors have proposed that a fluctuating rather than a static order order parameter is already sufficient to backfold the Fermi surface [49–53], or that short-range anti-ferromagnetic correlations may cause the pseudogap [54,55]. Hole pockets can also be produced by a phenomenological

ansatz for the self-energy [56], and it has also been proposed that the origin of the pseudogap is checkerboard-type CDW order [57]. On the other hand, one may also assume that there is no underlying free-electron Fermi surface that can be backfolded. Rather, in this picture the hole pockets are a consequence of the proximity to the Mott insulator, which corresponds to a nominally half-filled band but has no Fermi surface at all. The Hubbard-I approximation [58] predicts a hole pocket centered at (π, π) in a paramagnetic and translationally invariant ground state, whereby the volume of the pocket increases monotonically with x. However, the increase is nonlinear in x, which seems counterintuitive. The Hubbard-I approximation can be reformulated as a theory for holelike and doublonlike quasiparticles, which results in hole pockets with a volume that is strictly $\propto x$, and if short-range antiferromagnetic spin correlations are incorporated, the pocket indeed is centered near $(\frac{\pi}{2}, \frac{\pi}{2})$ [59]. Another such theory is the quantum dimer model proposed by Punk *et al.* [60–62], and the theory to be outlined below has some similarity to this theory. More precisely, in the following we apply bond particle theory to the *t-J* model. This was proposed by Sachdev and Bhatt [46] and applied subsequently to spin ladders [63–65], bilayers [66,67], intrinsically dimerized spin systems [68,69], and the "Kondo necklace" [70].

II. FORMALISM

A. Hamiltonian

We consider the *t-J* model on a two-dimensional (2D) square lattice with N sites, labeled by indices i, j and periodic boundary conditions. The Hamiltonian reads [71,72]

$$H = -\sum_{i,j} \sum_{\sigma} t_{i,j} \hat{c}^\dagger_{i,\sigma} \hat{c}_{j,\sigma} + J \sum_{\langle i,j \rangle} \mathbf{S}_i \cdot \mathbf{S}_j,$$

where $\hat{c}^\dagger_{i,\sigma} = c^\dagger_{i,\sigma}(1 - n_{i\bar{\sigma}})$, $\mathbf{S}_i$ is the operator of electron spin at site i, and $\langle i, j \rangle$ denotes a sum over all pairs of nearest neighbors. We assume that the hopping integrals $t_{i,j}$ are different from zero only for nearest [(1,0)-like], second-nearest [(1,1)-like], and third-nearest [(2,0)-like] neighbors, and we call the respective hopping integrals t, t', and t''. The nearest neighbor t will be taken as the unit of energy.

B. States of a single dimer

The basic idea of the calculation is to represent eigenstates of a single dimer by bond bosons (for even electron number) and bond fermions (for odd electron number). We consider a single dimer with the sites labeled 1 and 2 and first write down the four states with two electrons, which means the singlet and the triplet. Introducing the matrix 4-vector $\boldsymbol{\gamma} = (\tau_0, \boldsymbol{\tau})$ with $\tau_0 = 1$ and $\boldsymbol{\tau}$ the vector of Pauli matrices, the state 4-vector $\boldsymbol{\beta} = (s, \boldsymbol{t})$ is [46,63]

$$|\boldsymbol{\beta}\rangle = \frac{1}{\sqrt{2}} \sum_{\sigma,\sigma'} c^\dagger_{1,\sigma} (\boldsymbol{\gamma} i\tau_y)_{\sigma,\sigma'} c^\dagger_{2,\sigma'} |0\rangle. \tag{1}$$

The four states with a single electron can be classified by their parity and *z*-spin [64,68],

$$|f_{\pm,\sigma}\rangle = \frac{1}{\sqrt{2}} (c^\dagger_{1,\sigma} \pm c^\dagger_{2,\sigma})|0\rangle. \tag{2}$$

The last eigenstate is the empty dimer $|e\rangle = |0\rangle$. If the dimer is in one of the states with two electrons, (1), we consider it occupied by a boson, created by the operator 4-vector $(s^\dagger, \mathbf{t}^\dagger)$, whereas a dimer in one of the states (2) is considered occupied by a fermion, created by $f^\dagger_{\pm,\sigma}$. If the dimer is empty we again consider it occupied by a boson, created by $e^\dagger$. The states $|s\rangle$, $|f_{+,\sigma}\rangle$, and $|e\rangle$ are even under the exchange $1 \leftrightarrow 2$, whereas $|\mathbf{t}\rangle$ and $|f_{-,\sigma}\rangle$ are odd. We ascribe positive parity also to the operators $s^\dagger$, $f^\dagger_+$, and $e^\dagger$, and negative parity to $\mathbf{t}^\dagger$ and $f^\dagger_-$. The procedure to transcribe operators for the original *t-J* model to the representation in terms of bond particles is as follows: since the nine states introduced above form a complete basis of the Fock space of a dimer, any operator O acting within that dimer can be expressed as $\sum_{a,b} |a\rangle O_{a,b} \langle b|$, with $O_{a,b} = \langle a|O|b\rangle$. Replacing $|a\rangle\langle b| \to a^\dagger b$, we obtain an operator for the bond particles that has the same matrix elements as long as it is acting in the subspace of states with precisely one bond particle in the dimer. In this way, the representation of the spin operator at site $j \in \{1, 2\}$ becomes

$$\mathbf{S}_j \to \frac{\lambda_j}{2} (s^\dagger \mathbf{t} + \mathbf{t}^\dagger s) - \frac{i}{2} \mathbf{t}^\dagger \times \mathbf{t}$$
$$+ \frac{1}{4} (\mathbf{f}^\dagger_+ + \lambda_j \mathbf{f}^\dagger_-) \boldsymbol{\tau} (\mathbf{f}_+ + \lambda_j \mathbf{f}_-), \tag{3}$$

where $\lambda_j = (-1)^{j-1}$. Introducing the contravariant spinor $\mathbf{c} = (\hat{c}_\uparrow, \hat{c}_\downarrow)^T$, the representation of the electron annihilation operator at site j becomes

$$\mathbf{c}_j \to : \frac{1}{2} (s \, i\tau_y + \lambda_j \mathbf{t} \cdot \boldsymbol{\tau} i\tau_y)(\mathbf{f}^\dagger_+ - \lambda_j \mathbf{f}^\dagger_-)$$
$$+ \frac{1}{\sqrt{2}} e^\dagger (\mathbf{f}_+ + \lambda_j \mathbf{f}_-) :, \tag{4}$$

where : $\cdots$: denotes normal ordering. As mentioned above, these representations are valid in the subspace of states with precisely one bond particle in the dimer:

$$s^\dagger s + \mathbf{t}^\dagger \cdot \mathbf{t} + \sum_\sigma \sum_{\alpha \in \{\pm\}} f^\dagger_{\alpha,\sigma} f_{\alpha,\sigma} + e^\dagger e = 1. \tag{5}$$

C. Generalization to the plane

We now consider the original plane with N sites and assume that these are partitioned into $\frac{N}{2}$ disjunct dimers, whereby the sites in a dimer are always nearest neighbors. We call such a partitioning a dimer covering of the plane. Each dimer is assigned a dimer label $m \in \{1, 2, \ldots, N/2\}$. We consider a dimer with dimer label m, which consists of the sites i and j. When writing down the dimer states introduced above, we have to decide which of the two sites, i or j, corresponds to the site 1 and which one to the site 2 in (1) and (2). This is because some of the dimer states have negative parity under $1 \leftrightarrow 2$ so that their sign depends on this choice. We adopt the convention that for a bond in the *x*-direction (*y*-direction), the left (lower) site always corresponds to the site 1. We call the site that corresponds to 1 the 1-site and the site that corresponds to 2 the 2-site of the dimer. For each site i we define $\lambda_i = 1$ if it is the 1-site and -1 if it is the 2-site in its respective dimer. Next we introduce the bond particle operators defined above and give them an additional

dimer label, e.g., $s_m^\dagger$, $\mathbf{t}_m^\dagger$, or $f_{m,+,\uparrow}^\dagger$. Lastly, we define $\mathbf{R}_m = (\mathbf{R}_i + \mathbf{R}_j)/2$.

Next we derive the bond particle representation of the *t-J* Hamiltonian for the given dimer covering. The intradimer part of the Hamiltonian is

$$H_{\text{intra}} = \sum_m \left(-\frac{3J}{4} s_m^\dagger s_m + \frac{J}{4}\, \mathbf{t}_m^\dagger \cdot \mathbf{t}_m \right.$$

$$\left. - t \sum_\sigma (f_{m,+,\sigma}^\dagger f_{m,+,\sigma} - f_{m,-,\sigma}^\dagger f_{m,-,\sigma}) \right).$$

We proceed to the interdimer part of the Hamiltonian, which can be constructed using (3) and (4). Consider two dimers, *m* and *n*, and let there be a bond in the Hamiltonian that connects sites *i* and *j* such that site *i* belongs to dimer *m*, and site *j* to dimer *n*. Using (3) and (4), we then find the representations

$$J\,\mathbf{S}_i \cdot \mathbf{S}_j \to \frac{J\lambda_i\lambda_j}{4}(s_m^\dagger \mathbf{t}_m + \mathbf{t}_m^\dagger s_m)(s_n^\dagger \mathbf{t}_n + \mathbf{t}_n^\dagger s_n) - \frac{J}{4}\,(\mathbf{t}_n^\dagger \times \mathbf{t}_n)$$

$$\cdot (\mathbf{t}_m^\dagger \times \mathbf{t}_m) - \frac{iJ}{4}[\lambda_i(s_m^\dagger \mathbf{t}_m + \mathbf{t}_m^\dagger s_m) \cdot (\mathbf{t}_n^\dagger \times \mathbf{t}_n)$$

$$+ \lambda_j(s_n^\dagger \mathbf{t}_n + \mathbf{t}_n^\dagger s_n) \cdot (\mathbf{t}_m^\dagger \times \mathbf{t}_m)], \quad (6)$$

$$-t\sum_\sigma \hat{c}_{i,\sigma}^\dagger \hat{c}_{j,\sigma}$$

$$\to \frac{t}{4}\left[(s_m^\dagger s_n + \lambda_i\lambda_j \mathbf{t}_m^\dagger \cdot \mathbf{t}_n) \left(\sum_\sigma f_{n,j,\sigma}^\dagger f_{m,i,\sigma} \right) \right.$$

$$- (\lambda_i \mathbf{t}_m^\dagger s_n + \lambda_j s_m^\dagger \mathbf{t}_n) \cdot \mathbf{v}_{(n,j),(m,i)}$$

$$\left. - i\lambda_i\lambda_j(\mathbf{t}_m^\dagger \times \mathbf{t}_n) \cdot \mathbf{v}_{(n,j),(m,i)} \right], \quad (7)$$

where

$$f_{m,i,\sigma} = f_{m,+,\sigma} - \lambda_i f_{m,-,\sigma}, \quad (8)$$

and the vector $\mathbf{v}$ is defined as

$$\mathbf{v}_{(n,j),(m,i)} = \sum_{\sigma,\sigma'} f_{n,j,\sigma}^\dagger\, \boldsymbol{\tau}_{\sigma,\sigma'}\, f_{m,i,\sigma'}.$$

In (6) and (7) we have actually dropped all terms containing the boson $e_m^\dagger$, which represents the empty dimer, and also all terms originating from the second line in (3), which describes direct exchange between holes. The reason is that both the density of empty dimers and the contribution of direct exchange between holes should be $\propto x^2$, and we consider *x* to be small.

The factors of λ_i or λ_j in (6) and (7) guarantee the invariance of the Hamiltonian under symmetry operations of the lattice. A given dimer covering of the plane could, e.g., be rotated by $\frac{\pi}{2}$, and the bond particle Hamiltonian for the resulting dimer covering must be equivalent to the original one. Consider a bond pointing in the *y*-direction as in Fig. 1(a), which consists of the sites *i* and *j*. According to our convention, the site *i* is the 1-site so that the dimer state $|f_{-,\sigma}\rangle = (c_{i,\sigma}^\dagger - c_{j,\sigma}^\dagger)/\sqrt{2}$. Now assume the whole dimer covering is rotated counterclockwise by $\frac{\pi}{2}$. This is equivalent to a permutation of the numbers of the lattice sites, and we assume that thereby $i \to i'$ and $j \to j'$. The
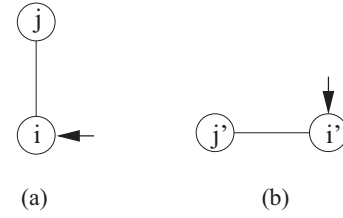

FIG. 1. Under a rotation by $\pi/2$ in the counterclockwise direction, the dimer in (a) is transformed into the one in (b). The arrow indicates the marked site.

transformed dimer state therefore is $(c_{i',\sigma}^\dagger - c_{j',\sigma}^\dagger)/\sqrt{2}$; see Fig. 1(b). However, according to our convention, the 1-site in the rotated dimer is j' so that the true dimer state is $|f_{-,\sigma}\rangle = (c_{j',\sigma}^\dagger - c_{i',\sigma}^\dagger)/\sqrt{2}$. The state $|f_{-,\sigma}\rangle$ thus acquires a factor of (-1) under this operation, and the same will hold true for any dimer state with negative parity. Now assume that one of the sites—say *i*—in the dimer is "marked" and consider the product $\lambda_i|f_{-,\sigma}\rangle$. The marked site in the rotated dimer then is i'. This is the 2-site in the rotated dimer so that $\lambda_{i'} = -1$ and the product $\lambda_i|f, -\rangle$ is invariant. This is easily seen to be general: any operation that exchanges the 1-site and the 2-site in a dimer inverts both the sign of a dimer state with odd parity and the sign of λ for the marked site, so that their product stays invariant. In (6) and (7) the marked sites are the ones where the Hamiltonian acts and the factors of λ are always associated with dimer states of negative parity.

When the hopping term contains longer-range hopping integrals such as t' and t'', it may happen that two bonds are connected by different hopping terms, as in Fig. 2. We consider the factors of λ in this case. Let us assume the nearest-neighbor term has $\lambda_i\lambda_j$ whereas the longer-range term has $\lambda_{i'}\lambda_{j'}$ as in Fig. 2. Now consider a symmetry operation of the lattice. If the operation exchanges the 1-site and the 2-site in bond *m*, both λ_i and $\lambda_{i'}$ change sign, whereas if the operation exchanges the 1-site and the 2-site in bond *n*, both λ_j and $\lambda_{j'}$ change sign. It follows that the products $\lambda_i\lambda_j$ and $\lambda_{i'}\lambda_{j'}$ always change sign "in phase" so that they are equal up to an overall sign. We define $\xi = \pm 1$ as the relative sign of the longer-range term with respect to the sign for nearest-neighbor hopping (or exchange): $\lambda_{i'}\lambda_{j'} = \xi\lambda_i\lambda_j$. ξ depends on the range of the hopping integral, and for t' and t'' terms one finds $\xi = -1$. For any two sites *i* and *j* we define $\xi_{i,j}$ to be this relative sign for the hopping term that connects them.

D. Approximations

The representation of the problem in terms of dimer states is exact but brings about no simplification so that
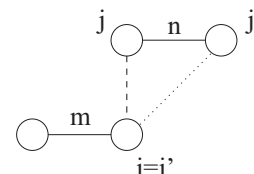

FIG. 2. Hopping terms of different range (dashed lines) connect two dimers in different ways.

approximations are necessary. As a first step, we reinterpret the singlet as the vacuum state of a dimer, and accordingly we replace the corresponding operators $s_m^\dagger$ and s_m in (6) and (7) by unity. This is equivalent to the assumption that as in a Mott insulator at half-filling, the electrons in the lightly doped Mott insulator form an inert background—the "singlet soup"—and that the only remaining active degrees of freedom are the spins of the electrons—represented by the triplets—and the doped holes, represented by the fermions. Replacing the singlet operators in (6) and (7) by unity, we obtain terms of second, third, and fourth order in triplet and fermion operators. The constraint (5) to have precisely one bond particle per dimer then becomes

$$\mathbf{t}_m^\dagger \cdot \mathbf{t}_m + \sum_{\alpha \in \{\pm\}} \sum_\sigma f_{m,\alpha,\sigma}^\dagger f_{m,\alpha,\sigma} + e_m^\dagger e_m \in \{0, 1\}, \qquad (9)$$

which must hold for each bond m. The constraint (9) is equivalent to an infinitely strong repulsive potential between bond particles in the same dimer. For small x, however, the density of triplets and fermions is small—this will be seen below and is crucial for the present theory. Namely, for Bose and Fermi systems of low density it is known that even such infinitely strong repulsive interactions between particles do not qualitatively change the ground state [73,74]. We therefore neglect the constraint assuming that it does not lead to a qualitative change of the results due to the low density of particles.

The problem with the infinitely strong repulsion between bond particles also occurs in the treatment of the Kondo lattice model. There it was found that good qualitative agreement with numerical results could be obtained by relaxing this constraint, and even quantitative agreement could be achieved by augmenting the energy of the bond particles by the loss of kinetic energy due to the blocking of bonds by a particle [75]. However, to keep the present treatment simple, we do not introduce this correction here. A more rigorous way to treat this repulsion has been carried out explicitly for bond bosons in spin systems by Kotov *et al.* [76] and Shevchenko *et al.* [77].

Even with the approximation to reduce the number of active degrees of freedom, we are far from a soluble problem because the theory still refers to a given dimer covering of the lattice, thus it is impossible to do any calculation for large systems. One might consider choosing a particular "simple" dimer covering. However, since one is forced to make approximations, the exactness of the dimer representation is lost and the special symmetry of the covering will make itself felt in the approximate solutions resulting, e.g., in an artificial supercell structure. On the other hand, the dimer Hamiltonian provides an exact representation of the original t-J model for *any* dimer covering of the plane. This means that, for example, the result for the spin correlation function $\langle \mathbf{S}_j(t) \cdot \mathbf{S}_i \rangle$ does not depend on the dimer covering in which the calculation is carried out. Put another way, the way in which a spin excitation propagates through the network of dimers from site $i \to j$ during the time t does not depend at all on the geometry of the dimer covering. This might suggest constructing a translationally invariant approximate Hamiltonian by *averaging* the dimer Hamiltonian over all possible coverings. This means that now every bond in the
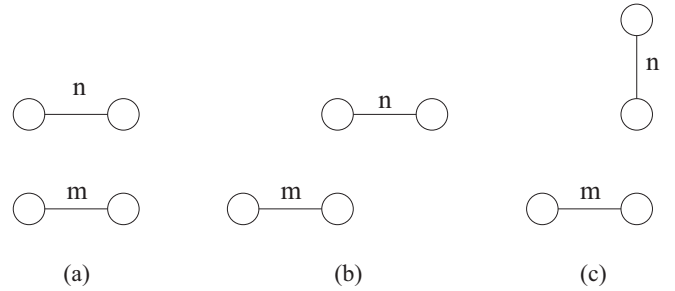

FIG. 3. Estimation of the renormalization factor ζ.

lattice may be occupied by a bond particle, and the averaged Hamiltonian for two bonds n and m is $\bar{h}_{n,m} = \zeta\, h_{n,m}$, where $h_{n,m}$ is given by the sum of (6) and (7), and

$$\zeta = \frac{N_{n,m}}{N_d}. \qquad (10)$$

Here $N_{n,m}$ is the number of dimer coverings that contain the bonds n and m, and N_d is the total number of dimer coverings. The resulting Hamiltonian is obviously translationally invariant and isotropic. To estimate ζ, we use a crude approximation: consider two adjacent bonds as in Fig. 3. By symmetry the bond m is covered by a dimer in exactly 1/4 of all dimer coverings, and we restrict ourselves to these. Assuming for simplicity that the number of coverings containing one of the three possible orientations of the adjacent bond n is equal, we estimate $\zeta = \frac{1}{12}$. Later on, it will be seen that, e.g., the spin gap depends sensitively on the value of ζ, and we will consider it as an adjustable parameter, but the values that give "reasonable" results are always around $\zeta = 0.1$.

In the averaged Hamiltonian there are additional unphysical configurations. For example, two bond particles may "cross" each other, see Fig. 4, and such configurations have to be excluded as well. This obviously amounts to an infinitely strong repulsion between the bond particles that acts whenever two bond particles share at least one site. Assuming the low-density limit, we neglect this repulsion.

Lastly, we discuss the operator of the electron number. If all dimers in a given covering are occupied by singlets or triplets, the number of electrons in the system is N. Each fermion reduces the number of electrons by 1, so if we discard the $e^\dagger$-boson,

$$x = \frac{1}{N} \sum_{m,\sigma} (f_{m,+,\sigma}^\dagger f_{m,+,\sigma} + f_{m,-,\sigma}^\dagger f_{m,-,\sigma}). \qquad (11)$$

Upon averaging, we increase the number of bonds that can be occupied by a particle from $N/2$ to $2N$. However, we retain the expression (11), which guarantees a Fermi surface with a volume proportional to the number of doped holes.
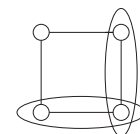

FIG. 4. Two "crossing" bond particles—such configurations are forbidden for the averaged Hamiltonian.

Lastly, we mention the convention for the Fourier transform of bond operators. Defining $\rho_{m,\alpha}$ (with $\alpha \in \{x, y\}$) to be 1 if m is a bond in the α-direction and 0 otherwise, the Fourier transform of a bond operator is (with $\alpha \in x, y$)

$$t_{\mathbf{k},\alpha}^{\dagger} = \frac{1}{\sqrt{N}} \sum_m \rho_{m,\alpha} \, e^{i\mathbf{k}\cdot\mathbf{R}_m} t_m^{\dagger}.$$

III. MEAN-FIELD THEORY

A. Mean-field decoupling

We next treat the bond particle Hamiltonian in Hartree-Fock approximation, thereby assuming a ground state that is invariant under spin rotations [46,63]. Accordingly, we drop the terms in (6) that are of third order in the triplets, and the terms in (7) that contain a single triplet or the vector product of two triplets. After Hartree-Fock decoupling, these terms would give expectation values such as $\langle \mathbf{t}_m \rangle$ or $\langle \mathbf{t}_m^{\dagger} \times \mathbf{t}_n \rangle$, which vanish in a spin-rotation invariant state. For better clarity, we give the remaining Hamiltonian after all approximations discussed so far have been made. The Hamiltonian is the sum of the following terms:

$$H_B^{(0)} = J \sum_m \mathbf{t}_m^{\dagger} \cdot \mathbf{t}_m + \frac{\zeta}{4} \sum_{m<n} \sum_{\substack{i\in m \\ j\in n}} J_{i,j} \lambda_i \lambda_j \, (\mathbf{t}_m^{\dagger} \cdot \mathbf{t}_n + \text{H.c.})$$

$$+ \frac{\zeta}{4} \sum_{m<n} \sum_{\substack{i\in m \\ j\in n}} J_{i,j} \lambda_i \lambda_j (\mathbf{t}_m^{\dagger} \cdot \mathbf{t}_n^{\dagger} + \text{H.c.}),$$

$$H_F^{(0)} = -t \sum_{m,\sigma} (f_{m,+,\sigma}^{\dagger} f_{m,+,\sigma} - f_{m,-,\sigma}^{\dagger} f_{m,-,\sigma})$$

$$+ \frac{\zeta}{4} \sum_{m,n} \sum_{\substack{i\in m \\ j\in n}} t_{i,j} \sum_{\sigma} f_{n,j,\sigma}^{\dagger} f_{m,i,\sigma},$$

$$H_B^{(1)} = -\frac{\zeta}{4} \sum_{m<n} \sum_{\substack{i\in m \\ j\in n}} J_{i,j} \, (\mathbf{t}_n^{\dagger} \times \mathbf{t}_n) \cdot (\mathbf{t}_m^{\dagger} \times \mathbf{t}_m),$$

$$H_{B,F}^{(1)} = \frac{\zeta}{4} \sum_{m,n} \sum_{\substack{i\in m \\ j\in n}} t_{i,j} \lambda_i \lambda_j \, \mathbf{t}_m^{\dagger} \cdot \mathbf{t}_n \sum_{\sigma} f_{n,j,\sigma}^{\dagger} f_{m,i,\sigma}. \quad (12)$$

Here $J_{i,j} = J$ if i and j are nearest neighbors and zero otherwise. $H_B^{(0)}$ and $H_F^{(0)}$ are the noninteracting parts for bosons and fermions, $H_B^{(1)}$ describes the interaction between bosons, and $H_{B,F}^{(1)}$ is the interaction between bosons and fermions. The double cross product in $H_B^{(1)}$ can be rewritten as

$$(\mathbf{t}_n^{\dagger} \times \mathbf{t}_n) \cdot (\mathbf{t}_m^{\dagger} \times \mathbf{t}_m)$$

$$= \sum_{\lambda \neq \lambda'} (t_{m,\lambda}^{\dagger} t_{n,\lambda}^{\dagger} \, t_{n,\lambda'} t_{m,\lambda'} - t_{m,\lambda}^{\dagger} t_{n,\lambda} \, t_{n,\lambda'}^{\dagger} t_{m,\lambda'}),$$

where $\lambda, \lambda' \in \{x, y, z\}$ denotes the spin of the triplet. Upon mean-field factorization and using the spin-rotation invariance of the ground state, this becomes [63]

$$\left(\tfrac{2}{3} \langle \mathbf{t}_m \cdot \mathbf{t}_n \rangle \, \mathbf{t}_m^{\dagger} \cdot \mathbf{t}_n^{\dagger} - \tfrac{2}{3} \langle \mathbf{t}_m^{\dagger} \cdot \mathbf{t}_n \rangle \, \mathbf{t}_n^{\dagger} \cdot \mathbf{t}_m \right) + \text{H.c.}$$

The expectation values of products of two triplet operators thereby take the form

$$\langle \mathbf{t}_m^{\dagger} \cdot \mathbf{t}_n \rangle = \lambda_i \, \lambda_j \, \theta_{m,n},$$

$$\langle \mathbf{t}_m \cdot \mathbf{t}_n \rangle = \lambda_i \, \lambda_j \, \eta_{m,n}, \quad (13)$$

where $i \in m$ and $j \in n$ are the sites where the exchange term acts and the "reduced expectation values" $\theta_{m,n}$ and $\eta_{m,n}$ are identical for all symmetry-equivalent pairs of bonds m, n. This follows from the fact that, e.g., $(\lambda_i \mathbf{t}_m) (\lambda_j \mathbf{t}_n)$ is symmetry invariant by construction. In the mean-field factorization of $H_{B,F}^{(1)}$ we again encounter the expectation values $\langle \mathbf{t}_m^{\dagger} \cdot \mathbf{t}_n \rangle$ and in addition fermionic expectation values. We define

$$\chi_{m,n} = \sum_{\substack{i\in m \\ j\in n}} \xi_{i,j} \frac{t_{i,j}}{t} \sum_{\sigma} \langle f_{m,i,\sigma}^{\dagger} f_{n,j,\sigma} \rangle. \quad (14)$$

Thereby, $\chi_{m,n}$ is the same for all symmetry-equivalent pairs of bonds m, n, which follows from the fact that $f_{m,\nu,\sigma}^{\dagger}$ in (8) is symmetry-invariant by construction. The symmetry properties of $\theta_{m,n}$, $\eta_{m,n}$, and $\chi_{m,n}$ can also be verified by performing a Hartree-Fock calculation *without* imposing any symmetry properties of the expectation values—it turns out that the self-consistent expectation values are always the same for all symmetry-equivalent bonds.

Upon decoupling the boson-fermion interaction term $H_{B,F}^{(1)}$ we obtain two separate problems, one for the bosons and the other for the fermions. The bosonic mean-field Hamiltonian is

$$H_B = J \sum_m \mathbf{t}_m^{\dagger} \cdot \mathbf{t}_m + \zeta \sum_{\langle m,n \rangle} [(\Delta_{m,n} \mathbf{t}_m^{\dagger} \cdot \mathbf{t}_n^{\dagger} + T_{m,n} \mathbf{t}_m^{\dagger} \cdot \mathbf{t}_n)$$
$$+ \text{H.c.}], \quad (15)$$

where $\langle m, n \rangle$ indicates a sum over all pairs of bonds m and n connected by a nearest-neighbor bond of the Hamiltonian, and

$$\Delta_{m,n} = \lambda_i \lambda_j \frac{J}{4} \left(1 - \frac{2}{3} \eta_{n,m}\right),$$

$$T_{m,n} = \lambda_i \lambda_j \left[\frac{J}{4} \left(1 + \frac{2}{3} \theta_{n,m}\right) + \frac{t}{4} \chi_{n,m} \right]. \quad (16)$$

Thereby $i \in m$ and $j \in n$ are the sites where the exchange term acts—these are necessarily nearest neighbors.

The fermionic mean-field Hamiltonian is (omitting the spin index for brevity)

$$H_F = -t \sum_m (f_{m,+}^{\dagger} f_{m,+} - f_{m,-}^{\dagger} f_{m,-}) + \zeta \sum_{m,n} \sum_{\substack{i\in m \\ j\in n}} \tilde{T}_{m,n}^{i,j} f_{m,i}^{\dagger} f_{n,j},$$

$$\tilde{T}_{m,n}^{i,j} = \frac{t_{i,j}}{4} (1 + \xi_{i,j} \theta_{n,m}). \quad (17)$$

Thereby, $\tilde{T}_{m,n}^{i,j}$ depends only on the type of hopping term (t, t' or t''), which connects the sites i and j and is the same for all symmetry-equivalent pairs of bonds m and n. Inserting (8), we find

$$f_{m,i}^{\dagger} f_{n,j} = f_{m,+}^{\dagger} f_{n,+} - \lambda_i f_{m,-}^{\dagger} f_{n,+}$$
$$- \lambda_j f_{m,+}^{\dagger} f_{n,-} + \lambda_i \lambda_j f_{m,-}^{\dagger} f_{n,-}.$$
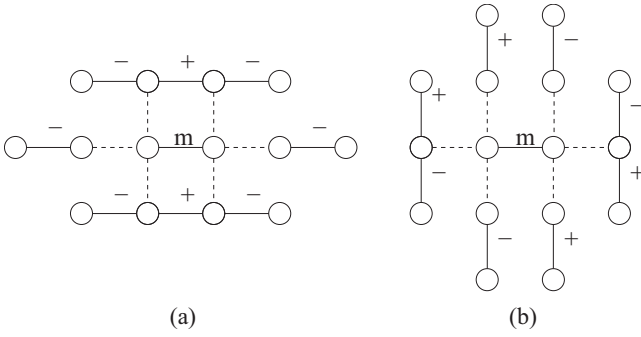
FIG. 5. The factors of $\lambda_i \lambda_j$ for all bonds connected to the bond m by the exchange term (dashed lines). In (a) both bonds are along the x-direction so that these pairs contribute to $\tilde{\epsilon}^{x,x}$ whereas in (b) one bond is along the y-direction so that these pairs contribute to $\tilde{\epsilon}^{x,y}$. In (a) both bonds connecting parallel bonds have $\lambda_i \lambda_j = 1$.

B. The bosonic problem

We consider H_B in (15). The parameters $\theta_{m,n}$, $\eta_{m,n}$, and $\chi_{m,n}$ are identical for all symmetry-equivalent pairs of bonds. In the following, we replace, e.g., $\theta_{m,n} \to \theta_{\mathbf{R}_m - \mathbf{R}_n}$, and the latter parameters are the same for all symmetry-equivalent distances. Fourier transformation of H_B then gives

$$H = \frac{1}{2} \sum_{\mathbf{k}} \sum_{\alpha,\beta \in \{x,y\}} \left(\mathbf{t}_{\mathbf{k},\alpha}^\dagger \Delta_{\mathbf{k}}^{\alpha,\beta} \mathbf{t}_{\beta,-\mathbf{k}}^\dagger + \text{H.c.} \right)$$
$$+ \sum_{\mathbf{k}} \sum_{\alpha,\beta \in \{x,y\}} \mathbf{t}_{\mathbf{k},\alpha}^\dagger \epsilon_{\mathbf{k}}^{\alpha,\beta} \mathbf{t}_{\beta,\mathbf{k}},$$

with the 2×2 matrices $\Delta_{\mathbf{k}}$ and $\epsilon_{\mathbf{k}}$ defined by

$$\Delta_{\mathbf{k}}^{\alpha,\beta} = \frac{1}{N} \sum_{m,n} \rho_{m,\alpha} \Delta_{m,n} \rho_{n,\beta} \, e^{i\mathbf{k}\cdot(\mathbf{R}_n - \mathbf{R}_m)}$$

and an analogous definition for $\epsilon_{\mathbf{k}}^{\alpha,\beta}$. We assume $\Delta_{m,n}$ and $T_{m,n}$ to be real so that $\epsilon_{-\mathbf{k}} = \epsilon_{\mathbf{k}}^*$ and $\Delta_{-\mathbf{k}} = \Delta_{\mathbf{k}}^*$. Both $\epsilon_{\mathbf{k}}$ and $\Delta_{\mathbf{k}}$ are Hermitian and $\epsilon_{\mathbf{k}} = J + \zeta \, \tilde{\epsilon}_{\mathbf{k}}$ with

$$\tilde{\epsilon}_{\mathbf{k}}^{x,x} = 4T_{(0,1)} \cos(k_y) - 2T_{(2,0)} \cos(2k_x)$$
$$- 4T_{(1,1)} \cos(k_x) \cos(k_y),$$
$$\tilde{\epsilon}_{\mathbf{k}}^{y,y} = 4T_{(1,0)} \cos(k_x) - 2T_{(0,2)} \cos(2k_y)$$
$$- 4T_{(1,1)} \cos(k_x) \cos(k_y),$$
$$\tilde{\epsilon}_{\mathbf{k}}^{x,y} = 4T_{(\frac{3}{2},\frac{1}{2})} \left[\sin\left(\frac{3k_x}{2}\right) \sin\left(\frac{k_y}{2}\right) \right.$$
$$\left. + \sin\left(\frac{k_x}{2}\right) \sin\left(\frac{3k_y}{2}\right) \right].$$

This can be verified using the signs of the products $\lambda_i \lambda_j$ in Fig. 5. The expressions for $\Delta_{\mathbf{k}}$ are obtained from those for $\tilde{\epsilon}_{\mathbf{k}}$

by replacing $T_{\mathbf{R}} \to \Delta_{\mathbf{R}}$. To diagonalize H, we make the ansatz

$$\tau_{\nu,\mathbf{k}}^\dagger = \sum_{\alpha \in \{x,y\}} (u_{\nu,\mathbf{k},\alpha} \, \mathbf{t}_{\mathbf{k},\alpha}^\dagger + v_{\nu,\mathbf{k},\alpha} \, \mathbf{t}_{-\mathbf{k},\alpha}),$$
$$\tau_{\nu,-\mathbf{k}} = \sum_{\alpha \in \{x,y\}} (v_{\nu,\mathbf{k},\alpha}^* \, \mathbf{t}_{\mathbf{k},\alpha}^\dagger + u_{\nu,\mathbf{k},\alpha}^* \, \mathbf{t}_{-\mathbf{k},\alpha}), \quad (18)$$

where $\nu \in \{1, 2\}$. Demanding $[\tau_{\nu,\mathbf{k}}, \tau_{\mu,\mathbf{k}}^\dagger] = \delta_{\nu,\mu}$ leads to

$$\sum_{\alpha \in \{x,y\}} (u_{\nu,\mathbf{k},\alpha}^* u_{\mu,\mathbf{k},\alpha} - v_{\nu,\mathbf{k},\alpha}^* v_{\mu,\mathbf{k},\alpha}) = \delta_{\nu,\mu}, \quad (19)$$

whereas $[H, \tau_{\nu,\mathbf{k}}^\dagger] = \omega_{\nu,\mathbf{k}} \tau_{\nu,\mathbf{k}}^\dagger$ results in the non-Hermitian eigenvalue problem

$$\begin{pmatrix} \epsilon_{\mathbf{k}} & -\Delta_{\mathbf{k}} \\ \Delta_{-\mathbf{k}}^* & -\epsilon_{-\mathbf{k}}^* \end{pmatrix} \begin{pmatrix} u_{\nu,k} \\ v_{\nu,k} \end{pmatrix} = \omega_{\nu,\mathbf{k}} \begin{pmatrix} u_{\nu,k} \\ v_{\nu,k} \end{pmatrix}. \quad (20)$$

For a matrix of the type on the left-hand side, it can be shown that the eigenvalues come in pairs of $\pm\omega$, and if (u, v) is the right eigenvector for $+\omega$, then (v^*, u^*) is the right eigenvector for $-\omega$—which justifies the ansatz (18). Moreover, $(u^*, -v^*)$ can be shown to be the left eigenvector for $+\omega$ so that (19) is equivalent to the condition that left and right eigenvectors for different eigenvalues are orthogonal—as it has to be. The mean-field Hamiltonian becomes

$$H_B = \sum_{\mathbf{k}} \left[\sum_{\nu=1}^{2} \omega_{\nu,\mathbf{k}} \left(\tau_{\nu,\mathbf{k}}^\dagger \, \tau_{\nu,\mathbf{k}} + \frac{3}{2} \right) - \frac{3}{2} \, \text{tr}(\epsilon_{\mathbf{k}}) \right],$$

and (18) can be reverted to give

$$\mathbf{t}_{\mathbf{k},\alpha}^\dagger = \sum_{\nu=1}^{2} (u_{\nu,\mathbf{k},\alpha}^* \, \tau_{\mathbf{k},\nu}^\dagger - v_{\nu,\mathbf{k},\alpha} \, \tau_{-\mathbf{k},\nu}),$$
$$\mathbf{t}_{-\mathbf{k},\alpha} = \sum_{\nu=1}^{2} (-v_{\nu,\mathbf{k},\alpha}^* \, \tau_{\mathbf{k},\nu}^\dagger + u_{\nu,\mathbf{k},\alpha} \, \tau_{-\mathbf{k},\nu}).$$

Using these expressions, the expectation values $\langle \mathbf{t}_{\mathbf{k},\alpha}^\dagger \cdot \mathbf{t}_{\mathbf{k},\beta} \rangle$ and $\langle \mathbf{t}_{\mathbf{k},\alpha} \cdot \mathbf{t}_{-\mathbf{k},\beta} \rangle$ can be obtained, from which the parameters $\theta_{m,n}$ and $\eta_{m,n}$ in (13) can be calculated.

C. The fermionic problem

We consider the fermionic Hamiltonian (17). Fourier transformation gives $H_F = \sum_{\mathbf{k}} H_{F,\mathbf{k}}$

$$H_{F,\mathbf{k}} = -t \sum_{\alpha \in \{x,y\}} (f_{\mathbf{k},\alpha,+}^\dagger f_{\mathbf{k},\alpha,+} - f_{\mathbf{k},\alpha,-}^\dagger f_{\mathbf{k},\alpha,-}) + \zeta \, v_{\mathbf{k}}^\dagger \tilde{H}_{\mathbf{k}} v_{\mathbf{k}},$$
$$(21)$$

where the vector $v_{\mathbf{k}} = (f_{k,x,+}, f_{k,y,+}, f_{k,x,-}, f_{k,y,-})^T$ has been introduced. Here we give the elements of the 4×4 matrix $\tilde{H}_{\mathbf{k}}$ for the case in which the t-J Hamiltonian contains only nearest-neighbor hopping:

$$\tilde{H}_{1,1} = 4\tilde{T}_{(0,1)} \cos(k_y) + 4\tilde{T}_{(1,1)} \cos(k_x) \cos(k_y) + 2\tilde{T}_{(2,0)} \cos(2k_x),$$
$$\tilde{H}_{1,2} = 4 \left[\tilde{T}_{(\frac{3}{2},\frac{1}{2})} \cos\left(\frac{3k_x}{2}\right) \cos\left(\frac{k_y}{2}\right) + \tilde{T}_{(\frac{1}{2},\frac{3}{2})} \cos\left(\frac{k_x}{2}\right) \cos\left(\frac{3k_y}{2}\right) \right],$$
$$\tilde{H}_{1,3} = -2i(2\tilde{T}_{(1,1)} \sin(k_x) \cos(k_y) + \tilde{T}_{(2,0)} \sin(2k_x)),$$

$$\tilde{H}_{1,4} = -4i\left[\tilde{T}_{(\frac{3}{2},\frac{1}{2})}\cos\left(\frac{3k_x}{2}\right)\sin\left(\frac{k_y}{2}\right) + \tilde{T}_{(\frac{1}{2},\frac{3}{2})}\cos\left(\frac{k_x}{2}\right)\sin\left(\frac{3k_y}{2}\right) \right],$$

$$\tilde{H}_{2,2} = 4\tilde{T}_{(1,0)}\cos(k_x) + 4\tilde{T}_{(1,1)}\cos(k_x)\cos(k_y) + 2\tilde{T}_{(0,2)}\cos(2k_y),$$

$$\tilde{H}_{2,3} = -4i\left[\tilde{T}_{(\frac{3}{2},\frac{1}{2})}\sin\left(\frac{3k_x}{2}\right)\cos\left(\frac{k_y}{2}\right) + \tilde{T}_{(\frac{1}{2},\frac{3}{2})}\sin\left(\frac{k_x}{2}\right)\cos\left(\frac{3k_y}{2}\right) \right],$$

$$\tilde{H}_{2,4} = -2i(2\tilde{T}_{(1,1)}\cos(k_x)\sin(k_y) + \tilde{T}_{(0,2)}\sin(2k_y)),$$

$$\tilde{H}_{3,3} = 4\tilde{T}_{(0,1)}\cos(k_y) - 4\tilde{T}_{(1,1)}\cos(k_x)\cos(k_y) - 2\tilde{T}_{(2,0)}\cos(2k_x),$$

$$\tilde{H}_{3,4} = 4\left[\tilde{T}_{(\frac{3}{2},\frac{1}{2})}\sin\left(\frac{3k_x}{2}\right)\sin\left(\frac{k_y}{2}\right) + \tilde{T}_{(\frac{1}{2},\frac{3}{2})}\sin\left(\frac{k_x}{2}\right)\sin\left(\frac{3k_y}{2}\right) \right],$$

$$\tilde{H}_{4,4} = 4\tilde{T}_{(1,0)}\cos(k_x) - 4\tilde{T}_{(1,1)}\cos(k_x)\cos(k_y) - 2\tilde{T}_{(0,2)}\cos(2k_y).$$

Note that on the respective right-hand sides we have used the notation $\tilde{T}_{m,n} \to \tilde{T}_{\mathbf{R}_m - \mathbf{R}_n}$ and dropped the superscripts on $\tilde{T}$ because they all refer to nearest neighbors. The terms in $\tilde{H}$ originating from longer-range hopping integrals such as t' and t'' are also easily written down, but the resulting expressions are lengthy so we do not give them here.

Diagonalizing $-(H_{F,\mathbf{k}} - \mu)$, we obtain the dispersion $E_{\nu,\mathbf{k}}$ (with $\nu = 1, \ldots, 4$) for the electronlike quasiparticles and the corresponding eigenvectors $\mathbf{e}_{\nu,\mathbf{k}}$, from which the mean-field expectation values $\chi_{n,m}$ (14) can be calculated. This allows us to perform the self-consistency procedure, thereby using Broyden's algorithm [78] for better convergence, and we obtain the self-consistent values of the bosonic parameters $\theta_{m,n}$ and $\eta_{m,n}$ in (13) and $\chi_{n,m}$ in (14).

D. Excitation spectra

Having obtained a self-consistent solution, we can evaluate physical properties such as the single-particle spectral function and the dynamic spin-structure factor. We consider a dimer m, which comprises the sites i and j. Using (3) and (4), one finds the following representations [63]:

$$\sum_{\nu\in\{i,j\}} e^{i\mathbf{k}\cdot\mathbf{R}_\nu}\ \hat{c}_\nu$$

$$\to e^{i\mathbf{k}\cdot\mathbf{R}_m} i\tau_y\left[\cos\left(\frac{k_\alpha}{2}\right) f^\dagger_{m,+} + i\sin\left(\frac{k_\alpha}{2}\right) f^\dagger_{m,-} \right]$$

$$-\mathbf{t}_m\cdot\boldsymbol{\tau} i\tau_y\left[\cos\left(\frac{k_\alpha}{2}\right) f^\dagger_{m,-} + i\sin\left(\frac{k_\alpha}{2}\right) f^\dagger_{m,+} \right],$$

$$\sum_{\nu\in\{i,j\}} e^{i\mathbf{k}\cdot\mathbf{R}_\nu}\ \mathbf{S}_\nu$$

$$\to -i\, e^{i\mathbf{k}\cdot\mathbf{R}_m}\left[\sin\left(\frac{q_\alpha}{2}\right)(\mathbf{t}^\dagger_m + \mathbf{t}_m) + \cos\left(\frac{q_\alpha}{2}\right) \mathbf{t}^\dagger_m\times\mathbf{t}_m \right], \tag{22}$$

where $\alpha \in \{x, y\}$ is the direction of the bond. Upon Fourier transformation, the respective second terms in both equations describe processes in which a triplet that is already present in the system is annihilated—since the momentum of the triplet is not fixed, this would result in incoherent continua. Accordingly, we drop these terms and retain only the first terms in both equations, which give δ-peaks. We have for any

operator O_i

$$\frac{1}{N}\sum_i e^{i\mathbf{k}\cdot\mathbf{R}_i} O_i = \frac{1}{4N}\sum_m\left(\sum_{i\in m} e^{i\mathbf{k}\cdot\mathbf{R}_i} O_i \right),$$

where $\sum_m$ denotes a sum over all nearest-neighbor bonds, and inserting (22) for the parenthetical term on the right-hand side gives

$$\hat{c}_{-\mathbf{k},\uparrow} = \frac{1}{4}\sum_{\alpha\in\{x,y\}}\left[\cos\left(\frac{k_\alpha}{2}\right) f^\dagger_{\mathbf{k},\alpha,+,\uparrow} + i\sin\left(\frac{k_\alpha}{2}\right) f^\dagger_{\mathbf{k},\alpha,-,\uparrow} \right],$$

$$S_\mathbf{q} = -\frac{i}{4}\sum_{\alpha\in\{x,y\}}\sin\left(\frac{q_\alpha}{2}\right)(\mathbf{t}^\dagger_{\mathbf{q},\alpha} + \mathbf{t}_{-\mathbf{q},\alpha}).$$

We then obtain the single-particle spectral function and the dynamic spin structure factor,

$$A(\mathbf{k}, \omega) = \sum_{\nu=1}^4 |e^*_{\nu,\mathbf{k}}\cdot a_\mathbf{k}|^2\delta(\omega - E_{\nu,\mathbf{k}}), \tag{23}$$

$$S(\mathbf{q}, \omega) = \int d\omega\, e^{i\omega t}\langle S_{-\mathbf{q}}(t)S_\mathbf{q}\rangle$$

$$= \sum_{\nu=1}^2 |F_\nu(\mathbf{q})|^2\delta(\omega - \omega_{\nu,\mathbf{q}}),$$

$$F_\nu(\mathbf{q}) = \sum_{\alpha\in\{x,y\}}\sin\left(\frac{q_\alpha}{2}\right)(u^*_{\nu,\mathbf{q},\alpha} - v^*_{\nu,\mathbf{q},\alpha}), \tag{24}$$

where $a_\mathbf{k} = (\cos(\frac{k_x}{2}), \cos(\frac{k_y}{2}), i\sin(\frac{k_x}{2}), i\sin(\frac{k_y}{2}))^T$. Using these expressions, the coherent spectral weight of the individual bands in the electron spectral function and spin structure factor can be calculated.

IV. RESULTS

Performing the self-consistency procedure described in the preceding section gives the self-consistent values of the mean-field parameters θ, η, and χ. Using these, the triplet frequencies $\omega_{\nu,\mathbf{q}}$ (with $\nu\in\{1,2\}$), the energies of the electronlike quasiparticles $E_{\nu,\mathbf{k}}$ (with $\nu\in\{1,\ldots,4\}$), and the excitation spectra can be calculated. The results presented below were obtained at inverse temperature $\beta = 200$.

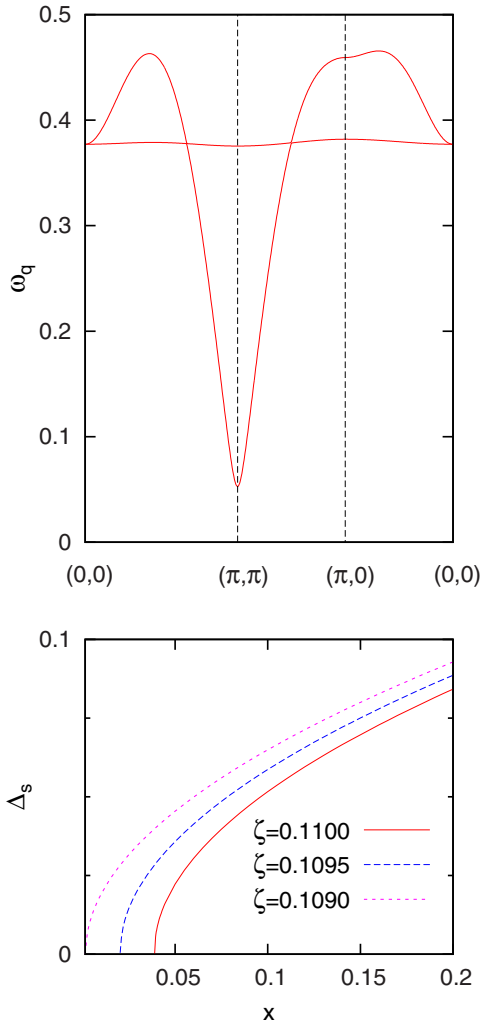FIG. 6. Top: triplet dispersion $\omega_{\nu,\boldsymbol{q}}$ [see (20)]. Parameter values are $J = 0.4$, $t' = t'' = 0$, $x = 0.1$, and $\zeta = 0.11$. Bottom: spin gap $\Delta_s = \omega_{(\pi,\pi)}$ vs x for different ζ, $J = 0.4$, $t' = t'' = 0$.

TABLE I. Self-consistent mean-field expectation values $\theta_{\mathbf{R}}$ and $\eta_{\mathbf{R}}$ in (13) and $\chi_{\mathbf{R}}$ in (14) for $J = 0.4$, $x = 0.1$, and $\zeta = 0.11$ whereby $t' = t'' = 0$ (A) and $t' = -0.2\, t'' = 0.1$ (B).

	A	B
$\theta_{(1,0)}$	-0.0234	-0.0233
$\theta_{(1,1)}$	-0.0198	-0.0196
$\theta_{(2,0)}$	-0.0229	-0.0228
$\theta_{(\frac{3}{2},\frac{1}{2})}$	-0.0223	-0.0221
$\eta_{(1,0)}$	-0.1178	-0.1176
$\eta_{(1,1)}$	-0.0673	-0.0672
$\eta_{(2,0)}$	-0.0720	-0.0718
$\eta_{(\frac{3}{2},\frac{1}{2})}$	-0.0712	-0.0710
$\chi_{(1,0)}$	-0.0330	-0.0210
$\chi_{(1,1)}$	-0.0347	-0.0356
$\chi_{(2,0)}$	-0.0110	0.0013
$\chi_{(\frac{3}{2},\frac{1}{2})}$	-0.0150	-0.0283

antiferromagnetic order sets in is unknown, we fix $\zeta = 0.11$ from now on.

Table I gives the values of the self-consistent parameters $\theta_{\mathbf{R}}$, $\eta_{\mathbf{R}}$, and $\chi_{\mathbf{R}}$. These are small so that for any approximate calculation at finite-doping—where the vanishing of Δ_S is of no concern—the self-consistent parameters could also be simply omitted. This was noted previously by Gopalan *et al.* in their study of spin-ladders [63]. Figure 7 shows some self-consistent mean-field parameters as a function of x and J. Except for a small range near the critical x where the spin gap closes, the bosonic parameters θ and η show little variation with either x or J. The fermionic parameter χ is linear in x as expected, and practically independent of J. Figure 8 shows the density of bosons per bond, n_B, and the combined density of bosons and fermions per bond, $n_B + \frac{x}{2}$, versus x. As already mentioned, the densities are small so that relaxing the various constraints on the bond particles may
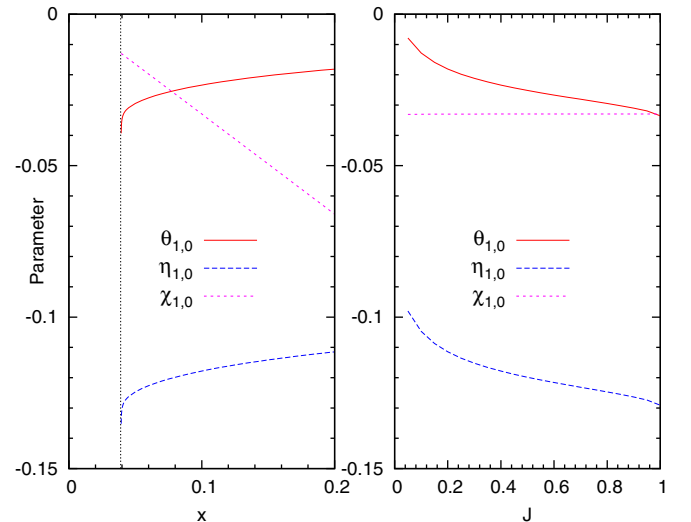
Figure 6 shows the dispersion $\omega_{\nu,\mathbf{q}}$ for the the triplet bosons. There is a dispersive band with a minimum at (π,π) and a second band with practically no dispersion. The coherent spectral weight $|F_\nu(\boldsymbol{q})|^2$ in the spin correlation function (24) vanishes for this band. Most likely this band therefore is an artefact of the enlargement of the basis of dimer particles in the course of the averaging procedure—an obvious drawback of the present approximation. The lower part of Fig. 6 shows the energy of the dispersive band at (π,π)—which we call the spin gap Δ_S—as a function of x. This is shown for different values of the parameter ζ, which originates in the averaging procedure. For larger x, Δ_S shows a roughly linear variation with x but bends down sharply as $x \to 0$ and reaches zero at a certain x, which depends sensitively on ζ. It is a plausible scenario that $\Delta_S \to 0$ for some small x, so that the triplets condense into momentum (π,π) resulting in antiferromagnetic order [46]. In this case, the triplet dispersion would be backfolded, resulting in a dispersion that is quite similar to that of antiferromagnetic magnons. The bandwidth, however, is only $\approx J$, whereas it should be $2J$, another deficiency of the present approximation. Since the precise value of x where

FIG. 7. Variation of mean-field parameters with x (for $J = 0.4$) and with J (for $x = 0.1$). The vertical line denotes the x where $\Delta_S \to 0$. Other parameter values are $t' = t'' = 0$, $\zeta = 0.11$.
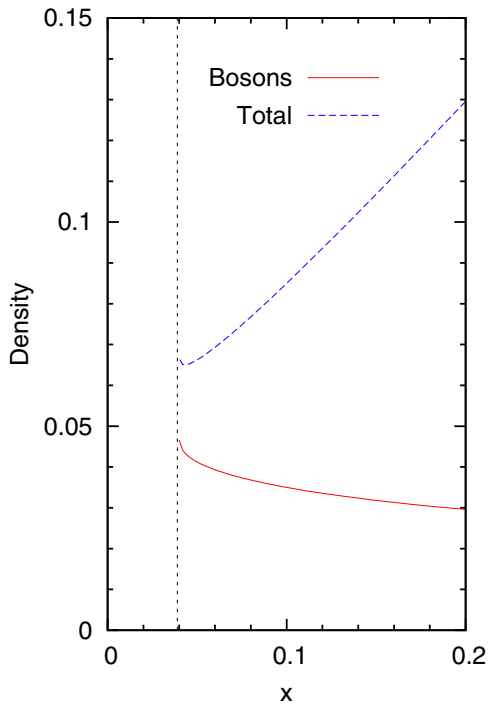
FIG. 8. Density of bosons and density of bosons and fermions per bond vs hole concentration x. The vertical line denotes the x where $\Delta_S \to 0$. Parameter values are $J = 0.4$, $t' = t'' = 0$, and $\zeta = 0.11$.

be reasonably justified. Figure 9 shows the band structure for electronlike quasiparticles, $E_{\nu,\mathbf{k}}$. The topmost band has a maximum between $(\frac{\pi}{2}, \frac{\pi}{2})$ and (π, π). For vanishing t' and t''
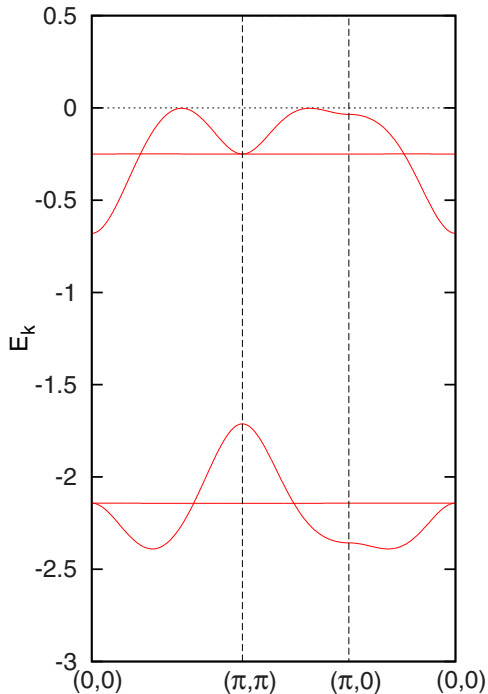

FIG. 9. Quasiparticle dispersion $E_{\nu,\mathbf{k}}$ [obtained by diagonalizing $-(H_{F,\mathbf{k}} - \mu)$ with $H_{F,\mathbf{k}}$ in (21)]. Parameter values are $J = 0.4$, $t' = t'' = 0$, $x = 0.1$, and $\zeta = 0.11$.
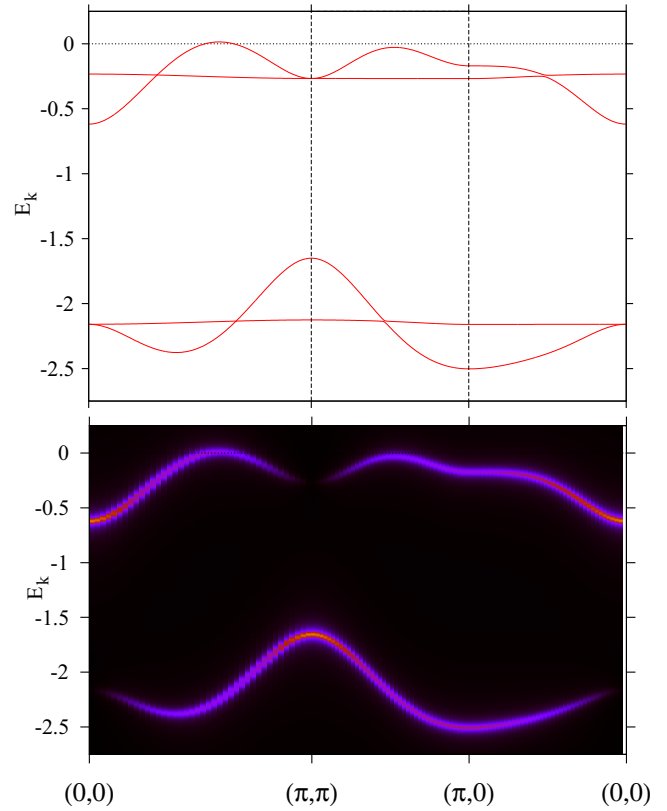

FIG. 10. Top: quasiparticle dispersion $E_{\nu,\mathbf{k}}$ for $J = 0.4$, $t' = -0.2$, $t'' = 0.1$, $x = 0.1$, and $\zeta = 0.11$. Bottom: corresponding spectral density $A(\mathbf{k}, \omega)$, see Eq. (23). δ-functions have been replaced by Lorentzians of width $\varepsilon = 0.02$.

this maximum is actually degenerate along a circular contour around (π, π), so that the fermi surface for finite x would be a ring with a tiny width around (π, π) (the area covered by the ring would be a fraction $x/2$ of the total Brillouin zone). This is obviously unphysical. In addition, there are two dispersionless bands at $\approx -0.25t$ and $\approx -2.14t$. As was the case for the dispersionless band in the triplet dispersion, these bands have zero coherent weight in the single-particle spectral function, so we again interpret them as being artefacts of the averaging procedure.

From now on we consider the system with additional longer-range hopping integrals $t' = -0.2$, $t'' = 0.1$, and $x = 0.1$. The self-consistent mean-field parameters for this case are also given in Table I. Figure 10 shows the band structure $E_{\nu,\mathbf{k}}$ and the single-particle spectral density $A(\mathbf{k}, \omega)$, while Fig. 11 displays the Fermi surface. Figure 10 confirms that the flat bands have no spectral weight—in fact, the spectral weight of these bands is not just small but zero to computer accuracy. Qualitatively, the topmost dispersive band that crosses μ can be compared to ARPES results in several aspects. Its maximum is at $(0.59\pi, 0.59\pi)$, so that the Fermi surface is a hole pocket centered at this point—see Fig. 11. The spectral weight of this band decreases as one moves toward (π, π) so that the outer edge of the pocket has a smaller spectral weight. However, the hole pocket is too close to (π, π) and the drop of spectral weight is far from being steep enough to really match experiment. Along
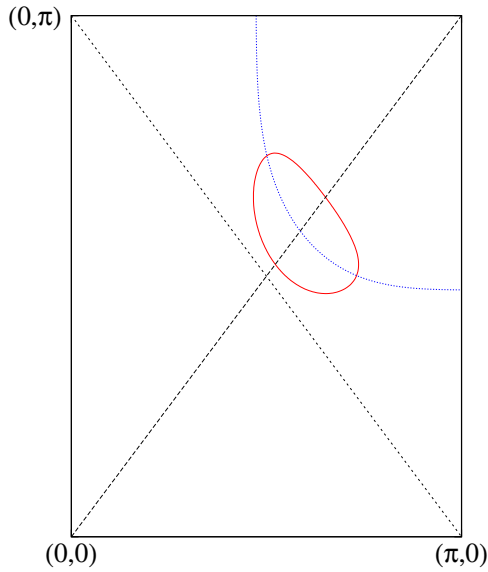
FIG. 11. Fermi surface for the parameter values in Fig. 10 (red). The blue line marks the maximum of the band as a function of the angle with respect to the line $(0, \pi) - (\pi, \pi)$.

$(\pi, 0) \to (\pi, \pi)$ the band first disperses toward μ. Then it bends down and loses weight around the bending point. This is qualitatively similar to the experiment in [10], but the bending point $(\pi, 0.47\pi)$ is too far from $(\pi, 0)$, the band is too far from μ at $(\pi, 0)$, and the drop of spectral weight is much too smooth. On the other hand, this is only the mean-field result, and coupling to the triplet bosons may lead to modifications of the quasiparticle dispersion and spectral weight, as is the case for hole motion in an antiferromagnet [79–83].

Figure 12 shows the triplet dispersion $\omega_{\nu, q}$ and the spectral intensity in the spin correlation function $S(\mathbf{q}, \omega)$. The dispersionless band has zero spectral weight, so that only a single mode is visible in $S(\mathbf{q}, \omega)$. This has a minimum at (π, π), and the spectral weight is concentrated sharply around this wave vector. Experimentally, inelastic neutron scattering from underdoped cuprates shows an "hourglass" or "X-shaped" dispersion around wave vector $\mathbf{q} = (\pi, \pi)$ [84] (which may also be "Y-shaped" [85]). This is frequently interpreted [84] as a magnonlike collective mode above the neck of the hourglass coexisting with particle-hole excitations of the Fermi gas of free carriers below the neck. The part above the neck of the hourglass thus would correspond to the triplet mode in Fig. 12. The mean-field treatment of the bond-particle Hamiltonian cannot reproduce the particle-hole excitations below the neck, but terms like $\mathbf{t}_n \cdot \mathbf{v}_{(n, \nu'), (m, \nu)}$ in (7), which describe the decay of a triplet into a particle-hole pair and which have been ignored in the mean-field treatment, may well produce these features. The mean-field triplet dispersion also does not reproduce the paramagnon excitations with $\mathbf{q}$ close to the zone center [86]. These paramagnons show a decreasing frequency as $\mathbf{q} \to \mathbf{0}$ [86], which differs strongly from the calculated $\omega_{\nu, q}$. On the other hand, in the mean-field approximation we have neglected anharmonic terms such as $\mathbf{t}_n^\dagger \cdot (\mathbf{t}_m^\dagger \times \mathbf{t}_m)$ in (6). By virtue of such terms, a magnon with momentum $\mathbf{q}$ close to the zone center may decay into two magnons with momenta $(\pi, \pi) + \mathbf{q}_1$ and $(\pi, \pi) + \mathbf{q} - \mathbf{q}_1$ with small $\mathbf{q}_1$ (coupled to a
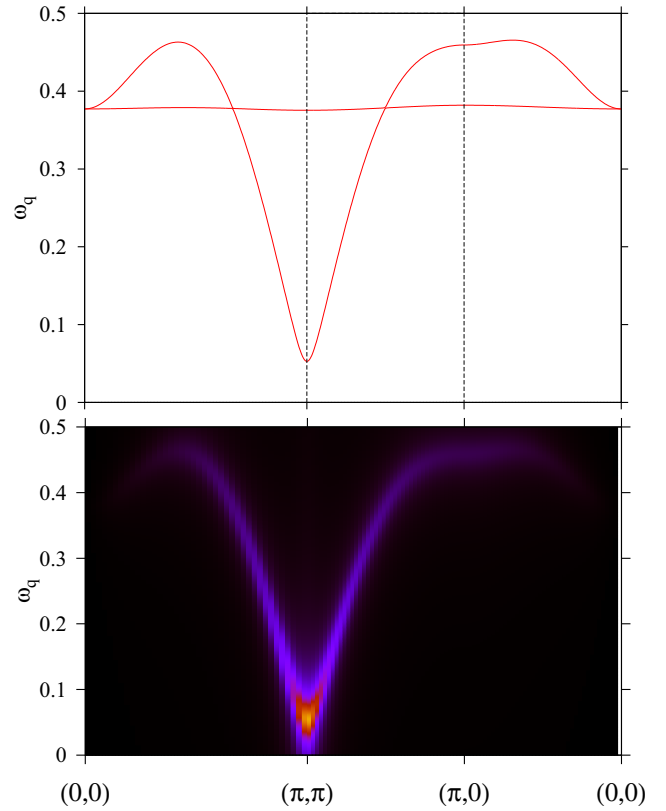

FIG. 12. Top: triplet dispersion $\omega_{\nu, q}$ [see (20)] for the parameter values in Fig. 10. Bottom: coherent spectral weight in the dynamic spin structure factor; see Eq. (24). δ-functions have been replaced by Lorentzians of width $\varepsilon = 0.02$.

triplet), and the true magnetic excitation may be a superposition of such states. We defer this to a separate study, however.

V. SUMMARY

In summary, we have presented a theory of the lightly doped paramagnetic Mott-insulator by formulating the t-J Hamiltonian in terms of bond particles for a given dimer covering of the plane, and averaging this over coverings. The major simplification for low doping thereby comes about because the majority of dimers are assumed to be in the singlet state, which we reinterpreted as the vacuum state of the dimer, so that a theory for a low-density system of holelike fermions and tripletlike bosons resulted. By virtue of the low density, relaxing the infinitely strong repulsion between these remaining particles may be a reasonable approximation. In fact, a similar approach has given reasonable results for the Kondo lattice, at least in the parameter range where the density of fermions and bosons indeed was small [75,87,88].

The results describe what might be expected for a doped Mott insulator after long-range antiferromagnetic order has collapsed: due to their strong Coulomb repulsion, the electrons are "jammed" so that the all-electron Fermi surface has collapsed. Instead, the electrons form an inert background— the "singlet soup"—and the only "active fermions" are the doped holes. These correspond to spin-$\frac{1}{2}$ fermions, and the fractional volume of the Fermi surface is $x/2$ rather than $(1 \pm x)/2$. As is the case in a Mott-insulator, the jammed electrons retain only their spin degrees of freedom, and the exchange

coupling between these results in a bosonic spin-triplet mode with a minimum at $\mathbf{q} = (\pi, \pi)$. The Fermi surface consists of hole pockets centered near $(\frac{\pi}{2}, \frac{\pi}{2})$ and symmetry-equivalent points. By and large, this description is consistent with a large body of experimental results for the pseudogap phase of underdoped cuprates, as discussed in the Introduction. It should be stressed that in order to obtain these results, use of the bond particle theory is advantageous. Namely, in the bond particle theory we have holelike spin-$\frac{1}{2}$ fermions (the $f_{m,\pm,\sigma}^{\dagger}$ fermions) and tripletlike spin excitations (the $\mathbf{t}_m^{\dagger}$ bosons) as the elementary excitations from the very outset. This can be contrasted, for example, with the slave-boson/fermion representation of the t-J model where one replaces $\hat{c}_{i,\sigma}^{\dagger} \rightarrow f_{i,\sigma}^{\dagger} b_i$, whereby the b-particle represents the empty site [89]. To model fermions that correspond to the doped holes, one would have to assign Fermi statistics to the b-particle, but then one would find spinless holes. On the other hand, the proportionality $S = aT\chi$ [22] suggests that the carriers in underdoped cuprates are spin-$\frac{1}{2}$ fermions.

Whereas the overall scenario predicted by the bond-particle theory is consistent with experiment, a more de-

tailed comparison shows clear deficiencies. Compared to experiment, the pocket is shifted toward (π, π) and the width of the quasiparticle band is too large. The $\mathbf{k}$-dependence of the spectral weight at the Fermi surface is too weak so that the spectral weight of the part of the pocket facing (π, π) is too large to actually reproduce the Fermi arcs. Moreover, the bandwidth of the triplet bosons is too small by a factor of ≈ 2. On the other hand, this is only the mean-field result, where moreover the infinitely strong repulsion between bond-particles has simply been neglected. Taking this into account as well as the coupling between holes and triplets may result in modifications. This can be seen from the reasonably well understood problem of hole motion in an antiferromagnet [79–83], where it is known that the hole is heavily dressed by spin fluctuations. For spin-ladders, the coupling between holes and triplets has already been carried out [64,65] in the framework of bond particle theory and given convincing results. Despite its obvious deficiencies, the bond particle formalism, therefore, may provide a reasonable starting point for more rigorous treatments of underdoped cuprates.

[1] B. Keimer, S. A. Kivelson, M. R. Norman, S. Uchida, and J. Zaanen, Nature (London) **518**, 179 (2015).

[2] A. G. Loeser, Z.-X. Shen, D. S. Dessau, D. S. Marshall, C. H. Park, P. Fournier, and A. Kapitulnik, Science **273**, 325 (1996).

[3] H. Ding, T. Yokoya, J. C. Campuzano, T. Takahashi, M. Randeria, M. R. Norman, T. Mochiku, K. Kadowaki, and J. Giapintzakis, Nature (London) **382**, 51 (1996).

[4] A. Damascelli, Z. Hussain, and Z.-X. Shen, Rev. Mod. Phys. **75**, 473 (2003).

[5] B. O. Wells, Z.-X. Shen, A. Matsuura, D. M. King, M. A. Kastner, M. Greven, and R. J. Birgeneau, Phys. Rev. Lett. **74**, 964 (1995).

[6] F. Ronning, C. Kim, D. L. Feng, D. S. Marshall, A. G. Loeser, L. L. Miller, J. N. Eckstein, L. Bozovic, and Z.-X. Shen, Science **282**, 2067 (1998).

[7] T. Kondo, A. D. Palczewski, Y. Hamaya, T. Takeuchi, J. S. Wen, Z. J. Xu, G. Gu, and A. Kaminski, Phys. Rev. Lett. **111**, 157003 (2013).

[8] H.-B. Yang, J. D. Rameau, Z.-H. Pan, G. D. Gu, P. D. Johnson, H. Claus, D. G. Hinks, and T. E. Kidd, Phys. Rev. Lett. **107**, 047003 (2011).

[9] K. Tanaka, W. S. Lee, D. H. Lu, A. Fujimori, T. Fujii, Risdiana, I. Terasaki, D. J. Scalapino, T. P. Devereaux, Z. Hussain, and Z.-X. Shen, Science **314**, 1910 (2006).

[10] M. Hashimoto, R.-H. He, K. Tanaka, J.-P. Testaud, W. Meevasana, R. G. Moore, D. Lu, H. Yao, Y. Yoshida, H. Eisaki, T. P. Devereaux, Z. Hussain, and Z.-X. Shen, Nat. Phys. **6**, 414 (2010).

[11] H. Eskes and R. Eder, Phys. Rev. B **54**, R14226(R) (1996).

[12] R. Eder and K. W. Becker, Phys. Rev. B **44**, 6982 (1991).

[13] O. P. Sushkov, G. A. Sawatzky, R. Eder, and H. Eskes, Phys. Rev. B **56**, 11769 (1997).

[14] J. M. Tranquada, B. J. Sternlieb, J. D. Axe, Y. Nakamura, and S. Uchida, Nature (London) **375**, 561 (1995).

[15] C. Howald, H. Eisaki, N. Kaneko, M. Greven, and A. Kapitulnik, Phys. Rev. B **67**, 014533 (2003).

[16] G. Ghiringhelli, M. Le Tacon, M. Minola, S. Blanco-Canosa, C. Mazzoli, N. B. Brookes, G. M. De Luca, A. Frano, D. G. Hawthorn, F. He, T. Loew, M. Moretti Sala, D. C. Peets, M. Salluzzo, E. Schierle, R. Sutarto, G. A. Sawatzky, E. Weschke, B. Keimer, and L. Braicovich, Science **337**, 821 (2012).

[17] S. I. Mirzaei, D. Stricker, J. N. Hancock, C. Berthod, A. Georges, E. van Heumen, M. K. Chan, X. Zhao, Y. Li, M. Greven, N. Barisic, and D. van der Marel, Proc. Natl. Acad. Sci. USA **110**, 5774 (2013).

[18] Y. Ando, Y. Kurita, S. Komiya, S. Ono, and K. Segawa, Phys. Rev. Lett. **92**, 197001 (2004).

[19] N. Barisic, M. K. Chan, Y. Li, G. Yu, X. Zhao, M. Dressel, A. Smontara, and M. Greven, Proc. Natl. Acad. Sci. USA **110**, 12235 (2013).

[20] G. Grissonnanche, F. Laliberte, S. Dufour-Beausejour, M. Matusiak, S. Badoux, F. F. Tafti, B. Michon, A. Riopel, O. Cyr-Choiniere, J. C. Baglo, B. J. Ramshaw, R. Liang, D. A. Bonn, W. N. Hardy, S. Kramer, D. LeBoeuf, D. Graf, N. Doiron-Leyraud, and L. Taillefer, Phys. Rev. B **93**, 064513 (2016).

[21] M. K. Chan, M. J. Veit, C. J. Dorow, Y. Ge, Y. Li, W. Tabis, Y. Tang, X. Zhao, N. Barisic, and M. Greven, Phys. Rev. Lett. **113**, 177005 (2014).

[22] J. W. Loram, K. A. Mirza, J. M. Wade, J. R. Cooper, N. Athanassopoulou, and W. Y. Liang, in *Advances in Superconductivity VII*, edited by K. Yamafuji and T. Morishita (Springer, Tokyo, 1995).

[23] S. Badoux, W. Tabis, F. Laliberte, G. Grissonnanche, B. Vignolle, D. Vignolles, J. Beard, D. A. Bonn, W. N. Hardy, R. Liang, N. Doiron-Leyraud, L. Taillefer, and C. Proust, Nature (London) **531**, 210 (2016).

[24] C. Collignon, S. Badoux, S. A. A. Afshar, B. Michon, F. Laliberte, O. Cyr-Choiniere, J.-S. Zhou, S. Licciardello, S. Wiedmann, N. Doiron-Leyraud, and L. Taillefer, Phys. Rev. B **95**, 224517 (2017).

[25] N. P. Ong, Z. Z. Wang, J. Clayhold, J. M. Tarascon, L. H. Greene, and W. R. McKinnon, Phys. Rev. B **35**, 8807 (1987).

[26] H. Takagi, T. Ido, S. Ishibashi, M. Uota, S. Uchida, and Y. Tokura, Phys. Rev. B **40**, 2254 (1989).

[27] W. J. Padilla, Y. S. Lee, M. Dumm, G. Blumberg, S. Ono, K. Segawa, S. Komiya, Y. Ando, and D. N. Basov, Phys. Rev. B **72**, 060511(R) (2005).

[28] J. Tallon and J. Loram, Physica C **349**, 53 (2001).

[29] N. Doiron-Leyraud, C. Proust, D. LeBoeuf, J. Levallois, J.-B. Bonnemaison, R. Liang, D. A. Bonn, W. N. Hardy, and L. Taillefer, Nature (London) **447**, 565 (2007).

[30] S. E. Sebastian, N. Harrison, M. M. Altarawneh, C. H. Mielke, R. Liang, D. A. Bonn, and G. G. Lonzarich, Proc. Natl. Acad. Sci. USA **107**, 6175 (2010).

[31] M. K. Chan, N. Harrison, R. D. McDonald, B. J. Ramshaw, K. A. Modic, N. Barisic, and M. Greven, Nat. Commun. **7**, 12244 (2016).

[32] C. Proust, B. Vignolle, J. Levallois, S. Adachi, and N. E. Hussey, Proc. Natl. Acad. Sci. USA **113**, 13654 (2016).

[33] D. LeBoeuf, N. Doiron-Leyraud, J. Levallois, R. Daou, J.-B. Bonnemaison, N. E. Hussey, L. Balicas, B. J. Ramshaw, R. Liang, D. A. Bonn, W. N. Hardy, S. Adachi, C. Proust, and L. Taillefer, Nature (London) **450**, 533 (2007).

[34] B. J. Ramshaw, B. Vignolle, J. Day, R. Liang, W. Hardy, C. Proust, and D. A. Bonn, Nat. Phys. **7**, 234 (2011).

[35] R. Comin, A. Frano, M. M. Yee, Y. Yoshida, H. Eisaki, E. Schierle, E. Weschke, R. Sutarto, F. He, A. Soumyanarayanan, Y. He, M. Le Tacon, I. S. Elfimov, J. E. Hoffman, G. A. Sawatzky, B. Keimer, and A. Damascelli, Science **343**, 390 (2014).

[36] R. Eder and Y. Ohta, Phys. Rev. B **51**, 6041 (1995).

[37] S. Nishimoto, Y. Ohta, and R. Eder, Phys. Rev. B **57**, R5590(R) (1998).

[38] D. L. Feng, N. P. Armitage, D. H. Lu, A. Damascelli, J. P. Hu, P. Bogdanov, A. Lanzara, F. Ronning, K. M. Shen, H. Eisaki, C. Kim, J.-i. Shimoyama, K. Kishio, and Z.-X. Shen, Phys. Rev. Lett. **86**, 5550 (2001).

[39] Y.-D. Chuang, A. D. Gromko, A. Fedorov, Y. Aiura, K. Oka, Y. Ando, H. Eisaki, S. I. Uchida, and D. S. Dessau, Phys. Rev. Lett. **87**, 117002 (2001).

[40] M. Plate, J. D. F. Mottershead, I. S. Elfimov, D. C. Peets, R. Liang, D. A. Bonn, W. N. Hardy, S. Chiuzbaian, M. Falub, M. Shi, L. Patthey, and A. Damascelli, Phys. Rev. Lett. **95**, 077001 (2005).

[41] N. E. Hussey, M. Abdel-Jawad, A. Carrington, A. P. Mackenzie, and L. Balicas, Nature **425**, 814 (2003).

[42] B. Vignolle, A. Carrington, R. A. Cooper, M. M. J. French, A. P. Mackenzie, C. Jaudet, D. Vignolles, C. Proust, and N. E. Hussey, Nature (London) **455**, 952 (2008).

[43] S. Nakamae, K. Behnia, N. Mangkorntong, M. Nohara, H. Takagi, S. J. C. Yates, and N. E. Hussey, Phys. Rev. B **68**, 100502(R) (2003).

[44] R. Eder and Y. Ohta, Phys. Rev. B **51**, 11683 (1995).

[45] R. Eder, Y. Ohta, and S. Maekawa, Phys. Rev. Lett. **74**, 5124 (1995).

[46] S. Sachdev and R. N. Bhatt, Phys. Rev. B **41**, 9323 (1990).

[47] S. Chakravarty, C. Nayak, and S. Tewari, Phys. Rev. B **68**, 100504(R) (2003).

[48] S. Chakravarty and H.-Y. Kee, Proc. Natl. Acad. Sci. USA **105**, 8835 (2008).

[49] Y. Qi and S. Sachdev, Phys. Rev. B **81**, 115129 (2010).

[50] E. G. Moon and S. Sachdev, Phys. Rev. B **83**, 224508 (2011).

[51] M. Punk and S. Sachdev, Phys. Rev. B **85**, 195123 (2012).

[52] M. Holt, J. Oitmaa, W. Chen, and O. P. Sushkov, Phys. Rev. Lett. **109**, 037001 (2012).

[53] M. Holt, J. Oitmaa, W. Chen, and O. P. Sushkov, Phys. Rev. B **87**, 075109 (2013).

[54] D. Senechal and A.-M. S. Tremblay, Phys. Rev. Lett. **92**, 126401 (2004).

[55] B. Kyung, S. S. Kancharla, D. Senechal, A.-M. S. Tremblay, M. Civelli, and G. Kotliar, Phys. Rev. B **73**, 165114 (2006).

[56] T. M. Rice, K.-Y. Yang, and F. C. Zhang, Rep. Prog. Phys. **75**, 016502 (2012).

[57] J.-X. Li, C.-Q. Wu, and D.-H. Lee, Phys. Rev. B **74**, 184515 (2006)

[58] J. Hubbard, Proc. R. Soc. London, A **276**, 238 (1964).

[59] R. Eder, P. Wrobel, and Y. Ohta, Phys. Rev. B **82**, 155109 (2010).

[60] M. Punk, A. Allais, and S. Sachdev, Proc. Natl. Acad. Sci. USA **112**, 9552 (2015).

[61] S. Huber, J. Feldmeier, and M. Punk, Phys. Rev. B **97**, 075144 (2018).

[62] J. Feldmeier, S. Huber, and M. Punk, Phys. Rev. Lett. **120**, 187001 (2018).

[63] S. Gopalan, T. M. Rice, and M. Sigrist, Phys. Rev. B **49**, 8901 (1994).

[64] O. P. Sushkov, Phys. Rev. B **60**, 3289 (1999).

[65] C. Jurecka and W. Brenig, Phys. Rev. B **63**, 094409 (2001).

[66] M. Vojta and K. W. Becker, Phys. Rev. B **60**, 15201 (1999).

[67] S. Ray and M. Vojta, Phys. Rev. B **98**, 115102 (2018).

[68] O. P. Sushkov, Phys. Rev. B **63**, 174429 (2001).

[69] K. Park and S. Sachdev, Phys. Rev. B **64**, 184510 (2001).

[70] M. Siahatgar, B. Schmidt, G. Zwicknagl, and P. Thalmeier, New J. Phys. **14**, 103005 (2014).

[71] K. A. Chao, J. Spalek, and A. M. Oles, J. Phys. C **10**, L271 (1977).

[72] F. C. Zhang and T. M. Rice, Phys. Rev. B **37**, 3759 (1988).

[73] V. M. Galitskii, Sov. Phys. JETP **7**, 104 (1958).

[74] S. T. Beliaev, Sov. Phys. JETP **7**, 299 (1958).

[75] R. Eder, Phys. Rev. B **99**, 085134 (2019).

[76] V. N. Kotov, O. Sushkov, Z. Weihong, and J. Oitmaa, Phys. Rev. Lett. **80**, 5790 (1998).

[77] P. V. Shevchenko, A. W. Sandvik, and O. P. Sushkov, Phys. Rev. B **61**, 3475 (2000).

[78] D. D. Johnson, Phys. Rev. B **38**, 12807 (1988).

[79] L. N. Bulaevskii, E. L. Nagaev, and D. L. Khomskii, Sov. Phys. JETP **27**, 836 (1968).

[80] S. A. Trugman, Phys. Rev. B **37**, 1597 (1988); **41**, 892 (1990).

[81] R. Eder and K. W. Becker, Z. Phys. B **78**, 219 (1990).

[82] G. Martinez and P. Horsch, Phys. Rev. B **44**, 317 (1991).

[83] W. Chen and O. P. Sushkov, Phys. Rev. B **88**, 184501 (2013).

[84] M. Fujita, H. Hiraka, M. Matsuda, M. Matsuura, J. M. Tranquada, S. Wakimoto, G. Xu, and K. Yamada, J. Phys. Soc. Jpn. **81**, 011007 (2012).

[85] M. K. Chan, C. J. Dorow, L. Mangin-Thro, Y. Tang, Y. Ge, M. J. Veit, G. Yu, X. Zhao, A. D. Christianson, J. T. Park, Y. Sidis, P. Steffens, D. L. Abernathy, P. Bourges, and M. Greven, Nat. Commun. **7**, 10819 (2016).

[86] M. Le Tacon, G. Ghiringhelli, J. Chaloupka, M. Moretti Sala, V. Hinkov, M. W. Haverkort, M. Minola, M. Bakr, K. J. Zhou, S. Blanco-Canosa, C. Monney, Y. T. Song, G. L. Sun, C. T. Lin, G. M. De Luca, M. Salluzzo, G. Khaliullin, T. Schmitt, L. Braicovich, and B. Keimer, Nat. Phys. **7**, 725 (2011).

[87] R. Eder, K. Grube, and P. Wróbel, Phys. Rev. B **93**, 165111 (2016).

[88] R. Eder and P. Wróbel, Phys. Rev. B **98**, 245125 (2018).

[89] P. A. Lee, N. Nagaosa, and X.-G. Wen, Rev. Mod. Phys. **78**, 17 (2006).